Hindawi
Advances in Civil Engineering
Volume 2019, Article ID 6401730, 8 pages
https://doi.org/10.1155/2019/6401730

Research Article

Experimental and Theoretical Research on Shear Strength of Seismic-Damaged SRC Frame Columns Strengthened with Enveloped Steel Jackets

Chengxiang C. X. Xu,[1] Peng S. Sheng ,[1] and Chong C. Wan[2]

[1]*School of Urban Construction, Wuhan University of Science and Technology, Wuhan 430065, China*
[2]*School of Urban Construction, Yangtze University, Jingzhou 434023, China*

Correspondence should be addressed to Peng S. Sheng; pe_sh@sina.com

Received 19 July 2018; Revised 14 September 2018; Accepted 11 December 2018; Published 3 January 2019

Academic Editor: Humberto Varum

The experimental and shear strength analytical investigations carried out on seismic-damaged steel reinforced concrete (SRC) columns strengthened with enveloped steel jacket subjected to cyclic loading are presented in this paper. Four 1/2-scale SRC columns were designed and manufactured and the postearthquake damage, enveloped steel jacket-confined, and destructive tests were carried out under lateral cyclic loading. The effects of postearthquake damage degree and enveloped steel jacket-confined on shear capacity and ductility capacity were all well examined. Test results indicate that the ductility of seismic-damaged SRC columns strengthened with enveloped steel jacket increases with the reduction of the postearthquake damage degree. The results indicate that the calculation formula of shear bearing capacity of SRC columns is feasible. Based on GB50010-2010, ACI318-08, and CSA-04, three different shear models were established, and the calculated values of shear capacity are quite different, and the analysis of the shear strength of RC in the strengthened seismic-damaged SRC column cannot be ignored. The formula is verified, and the calculated results are consistent well with the experimental results.

1. Introduction

As an attractive composite structure, SRC column structure has the advantages of high load-bearing capacity, excellent seismic performance, and so on [1]. Worldwide, SRC structures have been widely used in the areas that are prone to earthquakes [2]. However, research on seismic behavior of enveloped steel jacket-confined seismic-damaged SRC column has not been mentioned before. The impact of seismic damage and reinforcement on this kind of structure cannot be ignored, and it has very important engineering significance. In practical engineering, the mechanical properties of the enveloped steel jacket are excellent, because it is more convenient in construction [3]. The effective method of SRC structure reinforcement has been applied more and more widely in the USA, Canada, Japan and in Europe recently [4, 5]. Hence, for existing concrete structures, a thorough evaluation of seismic-damaged SRC columns which confined with enveloped steel jacket need to mitigate shear failure under earthquake loading, whereas for new concrete structures, the confined columns must be designed with sufficient shear capacity to sustain the whole building in an earthquake [6–8]. The purpose of this paper is to establish a model for predicting the shear strength of enveloped steel jacket restrained columns.

Compared with ordinary concrete column, RC columns with enveloped steel jacket have different seismic behavior [9–11]. In recent years, the seismic behavior of the seismic-damaged RC columns constrained by the enveloped steel jacket has been widely popularized, thus popularizing the use of enveloped steel jacket-confined concrete structure in earthquake regions. Nagaprasad et al. [12] presented the results obtained in the full-scale laboratory tests carried out on RC columns strengthened with steel cages. Garzón-Roca et al. [13] summarized some experimental researches on shear behavior of structures. Zhou et al. [14] indicated that

under low cyclic loading, the seismic performance of columns after strengthened can reach or even exceed that of the original column within a certain extent of the damage level. Fang et al. [15] tested the shear strength and the seismic behavior of concrete-encased steel cross-shaped columns submitted to a constant axial load and cyclic lateral loads.

Existing studies mainly concentrate on the flexural performance of strengthened SRC columns under lateral cyclic loading, but little information can be used to study the shear behavior of strengthened SRC column. Some post-earthquake reconnaissance has indicated that strengthened SRC columns are easily shear failure. To research the shear strength carried out on seismic-damaged SRC columns strengthened with enveloped steel jacket, four 1/2-scale SRC columns were designed and manufactured under the combined action of an axial load and reverse circulation lateral displacement. What's more, the seismic performance of enveloped steel jacket-confined SRC columns was evaluated. The proposed model was mainly used to analyze the shear strength of seismic damage degree and enveloped steel jacket reinforcement of specimen, and the rationality of the shear design codes [15–17] of the strengthened SRC columns need to be evaluated in the text.

2. Research Significance

To research the shear behavior of enveloped steel jacket-confined seismic-damaged SRC column, two main objectives were planned simultaneously to conduct the cover-all experimental program. The first objective includes making two different influence parameters for direct comparisons of seismic behavior of columns and providing new test data to the enveloped steel jacket-confined seismic-damaged SRC columns. The second objective is mainly to evaluate the effectiveness and applicability of the proposed modes.

3. Experimental Program

3.1. Specimen Design. Four SRC frame columns were constructed to investigate the seismic performance of seismic-damaged SRC frame columns confined with enveloped steel jacket. The test consisted of postearthquake damage loading, rehabilitation with enveloped steel jacket, and destructive tests under lateral cyclic loading. Column consisted of a 200 mm × 270 mm × 1150 mm column cast integrally and a 400 mm × 500 mm × 1000 mm foundation beam, which are shown in Figure 1. For all columns, the longitudinal bar ratio, ρ_l, was equal to 1.60%, the hoop ratio, ρ_{sv}, was equal to 0.68%, and the section steel ratio, ρ_a, was equal to 4.84%. Hoop spacing was 100 mm. The SRC column was a short column.

Two main parameters of the seismic performance of the column were researched: postearthquake damage degree of specimen and enveloped steel jacket confined or unconfined. SRC-0 specimen is undamaged or named original specimen and unconfined. WSRC-0 specimen is undamaged and confined. A displacement angle of 1/100 was used to simulate the moderate damage of specimen WSRC-1, while a displacement angle of 1/50 was used to simulate the severe damage of specimen WSRC-2. Axial compression ratio, n, of all specimens is 0.32, and shear span ratio, λ, is 3.33. Postearthquake damage degree of specimen includes three parts: undamaged, moderately damaged, and severely damaged. Angle steel was selected as 4L63 × 4, and the steel plate was selected in two sizes: 240 mm × 60 mm × 4 mm and 170 mm × 60 mm × 4 mm. Angle steel and steel plate are welding the enveloped steel jacket, which is filled with sticky steel glue as connecting with concrete. The spacing of adjacent steel plate is 150 mm, and reinforcement height is 500 mm.

3.2. Material Properties. The SRC column formulation based on a water-binder ratio of 0.39, and concrete cover was 25 mm. The compressive strength of concrete, f_{cu} (150 mm × 150 mm × 150 mm), of the specimen was 39.6 MPa. The compressive strength, f_c, was equal to $0.76f_{cu}$ [16]. The diameter of longitudinal bar was equaled to 16 mm, the yield stress, f_y, of longitudinal bar was 376 MPa, and the ultimate stress, f_u, was 515.6 MPa. The diameter of hoop was equaled to 8 mm, and the yield stress, f_{vy}, of hoop was 312 MPa, the ultimate stress, f_u, of hoop was 443.1 MPa. The yield stress, f_y, of I16 section steel was 264.5 MPa, and the ultimate stress, f_u, was 405.8 MPa.

3.3. Postearthquake Damage and Reinforcement of Specimens. The specimen SRC-0, with reinforcement, and the specimen WSRC-0, without any reinforcement, are undamaged. Displacement angle of 1/100 was used to simulate moderate damage of specimen WSRC-1, while a displacement angle of 1/50 was used to simulate severe damage of specimen WSRC-2. The angle steel and the steel plate are very important reinforcement materials and can form the envelope steel jacket by welded through the electric welding, which can be used to reinforce the specimen.

According to "Regulation of building seismic strengthening technique" (JGJ 138-01) [17], the size of angle steel and steel plate, the viscose method of concrete and enveloped steel jacket, the connection of enveloped steel jacket and ground beam, etc., are all consistent with parameters and methods shown by Xu et al. [18]. Angle steel extends to the ground beam and integral pouring [19]. The welding plate was welded with angle steel. Enveloped steel jacket was bonded with the concrete on the surface of the specimen through the structural adhesive. The specimen strengthened with enveloped steel jacket is shown in Figure 1.

3.4. Test Setup. The foundation beam was completely fixed. The top of the column was allowed to move. The lateral load was implemented at the top of the specimen through double-action actuator with displacement and force control capabilities. The axial load was applied all the time on the centroid of the free end section of the column and kept constant throughout the test. The sliding system consisted of thickness steel plate and pulley and kept frictional coefficient small enough. The test device is illustrated in Figure 2.

The tests of the loading system followed the JGJ 138-01 guidelines [17]. The loading system is shown in Figure 3. In

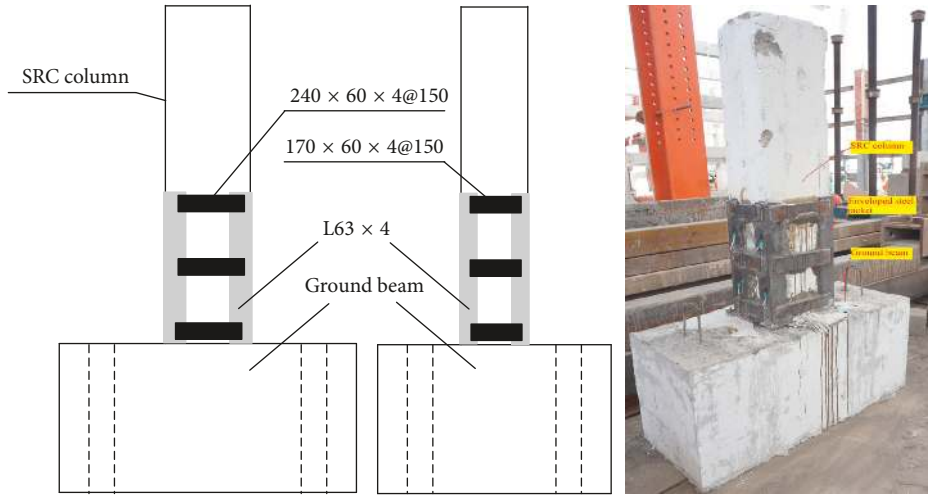

Figure 1: Enveloped steel jacket confined at column bottom.

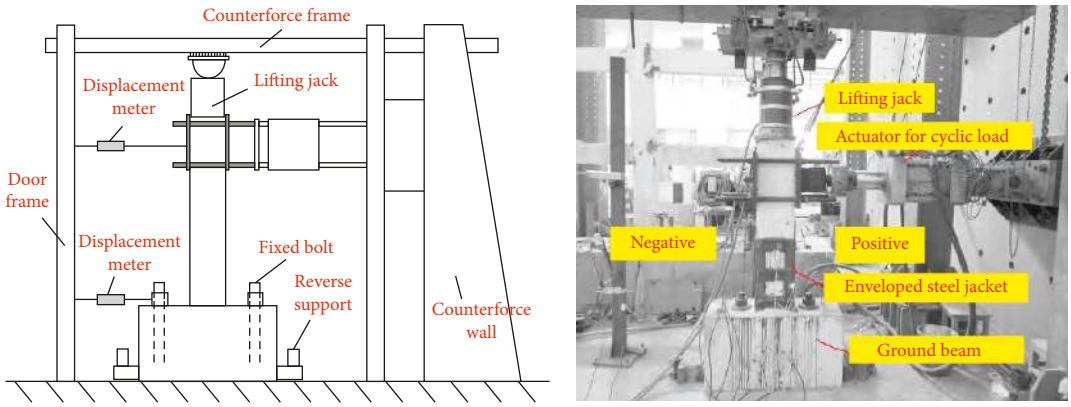

Figure 2: Test setup showing specimens.

the test, the target value of the axial load applied to maintain constantly by adjusting the hydraulic jack. The yielding displacement ($/L \times 100\% = 1.0\%$) is consistent with Xu et al. [18]. Both the initial applied horizontal load and each load step of the increment were 0.25%. The yield point is employed in this study to describe the obvious change of the slope of the shear force-displacement curve. All cycles were carried out once under the force control loading procedure [20]. The displacement amplitude increment was 1.0% [18]. All cycles were repeated three times for each amplitude. The specimens were subjected to three successive cycles after yielding, and the increments of 1.0% for each loading step. Two cases of test stop include, that is, the load is reduced to 0.85 times the limit load and the specimen axial failure.

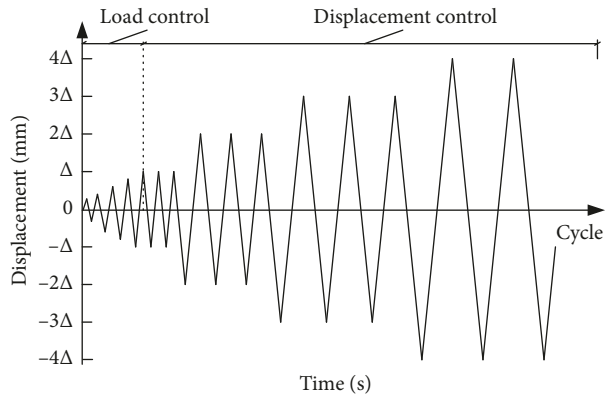

Figure 3: Loading protocols of the test.

3.5. Failure Modes and Damage Progression. A conceptual representation of three failure modes of column using displacement ductility versus shear force diagram [21] is shown in Figure 4. In the experiment, both flexural-shear failure and shear failure (showed in Figure 4) are regarded as the shear failure.

As the lateral force increased, the number and width of the diagonal cracks propagated. Moreover, as the postearthquake damage degree increased and enveloped steel jacket confined, the value of the lateral displacement became smaller. With the lateral displacement further propagating, the concrete cover at the bottom of the specimen was flake-off when stiffness was

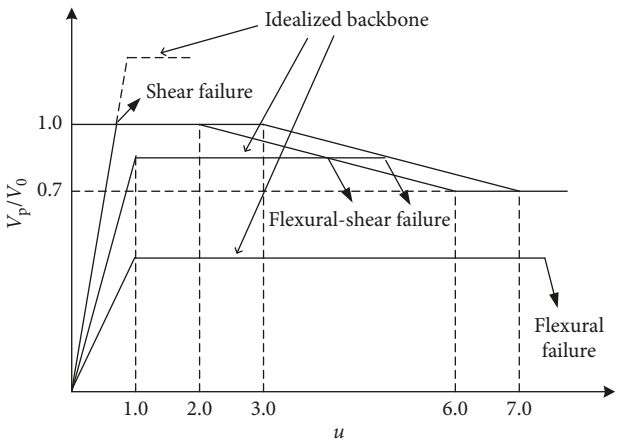

Figure 4: Definition of column failure modes.

gradually degrading, and this section was decreasing. Damage propagation and failure modes referenced [18].

The concrete of the shear-compression zone was crushed, whereas the combined action of compression and shear occurred. Fracture surfaces of SRC specimen needed to be well versed in the quite smooth because of the inclined cracks through the coarse aggregate. Figure 5 shows the failure mode of all specimens.

4. Experimental Results and Analysis

4.1. Hysteretic Curves and Backbone Curves. The skeleton curves of specimens are shown in Figure 6. From Table 1, compared with specimen SRC-0, the average of the ultimate load of WSRC-0 increased by 23.0% and the average of the ultimate displacement increased by 23.7% (consistent with Xu et al. [18]); the average of the ultimate load of WSRC-1 increased by 12.9% and the average of the ultimate displacement increased by 12.4%; and the average of the ultimate load of WSRC-2 increased by 7.4% and the average of the ultimate displacement increased by 8.0%.

Backbone curves shown in Figure 6 are not symmetric about the origin, because of some residual deformation after the forward cyclic loading. It was necessary to counteract the residual deformation caused by the forward cyclic loading when the reverse loading was applied.

Based on the theory of equivalent energy method, yield displacement and ultimate displacement are read from Figure 7, respectively. The feature points of the skeleton curve of the specimen are shown in Figure 6.

4.2. Ductility Coefficient. Ductility capacity is an important seismic parameter for structures, and ductility coefficient, μ, can be used to describe it:

$$\mu = \frac{\left|\Delta_u^+\right| + \left|\Delta_u^-\right|}{\left|\Delta_y^+\right| + \left|\Delta_y^-\right|}, \tag{1}$$

where Δ_u^+/Δ_u^- is the positive/negative ultimate displacement and Δ_y^+/Δ_y^- is the positive/negative yielding displacement.

The bearing capacity, deformation capacity and ductility coefficient of the specimen are listed in Table 1. The test results indicate that compared with the specimen SRC-0, the average ultimate bearing capacities of specimen WSRC-0 increased by 19.25% and the average limit displacement increased by 23.50%; the average ultimate bearing capacities of specimen WSRC-1 increased by 6.09% and the average limit displacement increased by 11.45%; and the average ultimate bearing capacities of test specimen WSRC-2 increased by 1.87% and the average limit displacement increased by 6.25%. The ductility coefficient of specimen WSRC-0 is increased by 17.6%; meanwhile, ductility coefficients of the specimen WSRC-1 and WSRC-2 are lowered to 11.4% and 10.4%, respectively. The ductility of seismic-damaged specimen can be effectively restored by enveloped steel jacket reinforcement.

4.3. Shear Strength of Specimens

4.3.1. Calculation of Shear Strength of Strengthened Columns. Wei and Zhang [22] developed the traditional truss-arch model. When the tests need to explore the shear bearing capacity of solid-webbed SRC short column, based on the truss-arch model, the solid-webbed SRC short column can divide SRC and section steel two parts to study. Lu et al. [23] provided the calculation method of sheer capacity of the strengthened column and considering the influence of enveloped steel jacket-confined (the influence of CFRP-confined ignored in this place). Hence, the proposed shear strength, V_m, of the seismic-damaged SRC columns confined with enveloped steel jacket can be expressed as

$$V_m = V_a + V_{cr} + V_g. \tag{2}$$

Based on the rules of the GB50010-2010, the ACI318-08, and the CSA-04, three different shear models were established, and the analysis of the shear strength of reinforcement seismic-damaged SRC column cannot be ignored [16, 24, 25]. Based on the rules of the GB50010-2010 [16], the RC column contribution, V_{cr}, is given by

$$V_{RC} = \frac{1.75}{\lambda + 1} f_t A + \rho_v f'_{yv} A + 0.07N, \tag{3aa}$$

where f_t is the design value of concrete axial tensile strength; ρ_v is the stirrup rate of column section; A is the effective area of the concrete section of seismic damage column.

Based on ACI318-08 [24], the RC column contribution, V_{cr}, is given by

$$\begin{aligned} V_{RC} &= V_C + V_S, \\ V_S &= \rho_v f'_{yv} A/b, \\ V_C &= \left(0.16\sqrt{f_c} + 17\rho_s \frac{V_{u1}A/b}{M_m}\right) A, \end{aligned} \tag{3ab}$$

where f_c is the axial compression strength of concrete; ρ_s is the reinforcement ratio of longitudinal reinforcement; $V_{u1}h_0/M_m$ is the the generalized shear span ratio of calculating section; h_0 is the effective height of column section.

Based on CSA-04 [25], the RC column contribution, V_{cr}, is given by

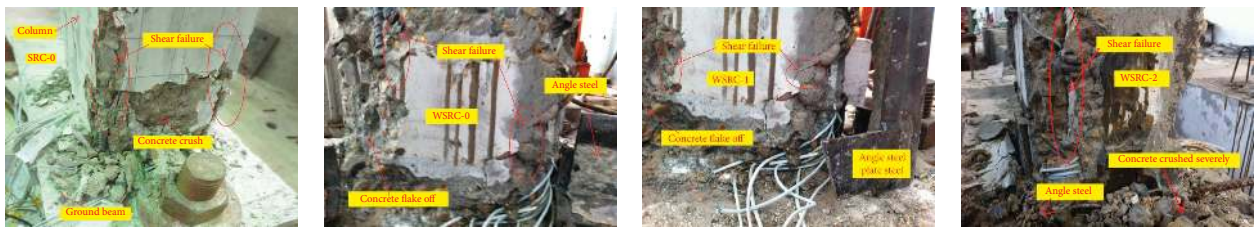

(a) (b) (c) (d)

Figure 5: Specimen failure. (a) SRC-0. (b) WSRC-0. (c) WSRC-1. (d) WSRC-2.

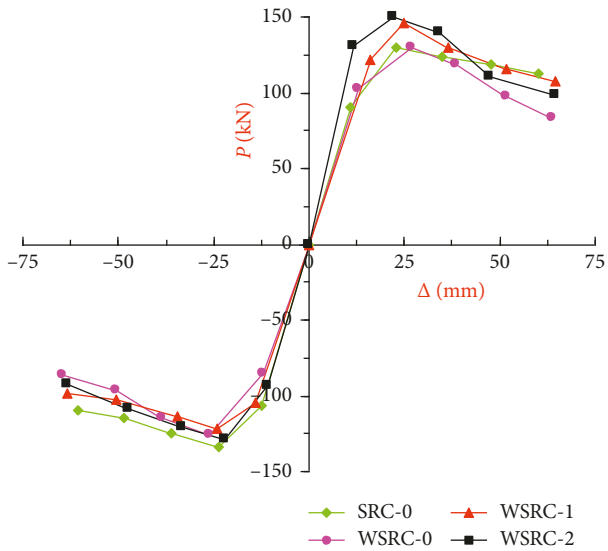

Figure 6: Backbone curves of specimens.

$$V_{RC} = \beta^* \sqrt{f_c} b d_v + \rho_v f'_{yv} d_v \cot\theta,$$

$$\beta^* = \frac{0.4}{1 + 1500\varepsilon_x} \cdot \frac{1300}{1000 + s_{ze}}, \tag{3ac}$$

$$\theta = 29 + 7000\varepsilon_x,$$

where β^* is the contribution coefficient of concrete; d_v is the longitudinal reinforcement diameter; f_c is the axial compression strength of concrete.

The enveloped steel jacket contribution, V_g, is given by equation (3b) [23]. The section steel contribution, V_a, is given by equation (3c) [22]:

$$V_g = v_g \rho_{sv} f_g b h_0, \tag{3b}$$

$$V_a = \frac{0.58 f_a t_w h_w}{\lambda - 0.2}, \tag{3c}$$

where f_{yv} is the yield stress of hoop; A_{sv} is the gross area of hoop; ρ_{sv} is the hoop ratio; s is the hoop spacing; f_g is the yield stress of enveloped steel jacket; N is the the axial load; t_w and h_w are the section steel thickness and height, respectively, and f_a is the the original strength of section steel before postearthquake damage of test columns. And the shear coefficient, v_g, can be computed by equation (4) [26, 27]:

$$v_g = \frac{1.639 \cdot (0.27 + 0.09\lambda - 0.13n)}{\sqrt{\rho_g f_{gt}/f_t} + 1.207}. \tag{4}$$

The tensile strength, f_t, needs to be redefined because the constraint action of the enveloped steel jacket is simplified to be the same as the restraint of the hoop. f_t [23, 28] is expressed as

$$f_t = 0.33\left[f_c + k_1\left(1 - \frac{x^2 + y^2}{36h}\right)\left(\frac{A_{sv}E_{sv}\varepsilon_{sv}}{sh_1} + \frac{A_z E_z \varepsilon_z}{s_z h}\right)\right]^{2/3}, \tag{5}$$

where x and y are the width and height of the effective restraint area of concrete, respectively. h_1 is the height of enveloped steel jacket-confined; A_z is the angle steel area; s_z is the plate spacing; E_{sv} and E_z are the modulus of elasticity of the hoop and enveloped steel jacket, respectively, ε_{sv} and ε_z are the effective strain of hoop and enveloped steel jacket, respectively.

However, based on the area of the section columns tested by Lu [29], Zhang [30], and Liu [31] that the area of the postearthquake damaged columns is not equal to bh_0. To solve the problem, Yang [14] gave a simplified method to calculate the strength of the hoop, longitudinal reinforcement, and section steel after earthquake damage. Divided, the column section consists of two parts with hoop as boundaries: core-zone area, A_1, and non-core-zone area, A_2, and the cross-sectional area of the column, A, is expressed as

$$A = 2(1 - D_1)bh_0 + a_F(h_0 - a_s)(b - 2a_s), \tag{6}$$

where D_1 is the damage index of the non-core-zone area of the section column $D_1 = 0.5$ for moderate damage and $D_1 = 1$ for severe damage. The strength reduction factor, a_F, can be computed by equation (7) [24]:

$$a_F = 1 + \beta_1 D + \beta_2 D^2, \tag{7}$$

where D is the damage index of specimen, which was proposed by Park–Ang in 1985 [32] and β_1 and β_2 are correlation coefficients and can be computed by the following equations [24]:

Table 1: Characteristic points of backbone curves.

Specimen	V_{cr} (kN)	V_y (kN)	$_y$ (mm)	V_u (kN)	$_u$ (mm)	V_{max} (kN)	$_{max}$ (mm)	μ ($_u$/ $_y$)	E
SRC-0	37.22	117.43 −119.11	16.45 −16.89	131.00 −133.01	47.67 −48.03	111.35 −113.06	26.80 −25.93	2.89 2.84	0.44
WSRC-0	44.32	140.19 −141.88	17.36 −17.41	161.14 −162.92	58.99 −59.17	136.97 −138.48	27.86 −28.01	3.40 3.40	0.53
WSRC-1	40.05	126.82 −124.12	16.64 −16.34	148.04 −143.89	53.58 −53.08	125.83 −122.31	27.14 −26.94	3.22 3.25	0.49
WSRC-2	39.62	121.09 −119.87	16.60 −16.27	140.80 −138.76	51.46 −50.21	115.46 −117.95	27.02 −26.47	3.10 3.09	0.46

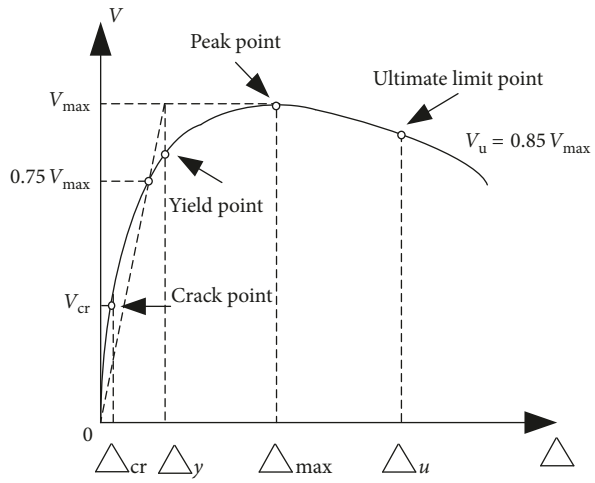

Figure 7: definition of displacement characteristic points.

$$\beta_1 = 0.127 - 0.000586 f'_{yv} + 0.229\left(\frac{f'_{yv}}{1000}\right)^2 + 0.00143 f_c, \tag{8a}$$

$$\beta_2 = -1.013 + 0.585n - 1.762n^2 + 0.183\rho_a + \frac{10.959}{f_c}. \tag{8b}$$

Yang [26] gave a simplified method to calculate the strength of the hoop, longitudinal reinforcement, and section steel after earthquake damage.

$$f'_{yv} = a_F f_{yv}, \tag{9a}$$

$$f'_{ck} = a_F f_{ck}, \tag{9b}$$

$$f'_a = a_F f_a, \tag{9c}$$

where f_{yv}, f_{ck}, and f_a is the original strength of hoop, longitudinal reinforcement, and section steel before post-earthquake damage of test columns, respectively, and f'_{yv}, f'_{ck}, and f'_a is the strength of the hoop, longitudinal reinforcement, and section steel after postearthquake damage of the test columns, respectively.

Therefore, equation (2) can be expressed as

$$V_{mu} = V_{au} + V_{cur,i} + V_{gu}, \tag{10}$$

where

$$V_{cur,GB} = \frac{1.75}{\lambda + 1} f_t A + \rho_v f'_{yv} A + 0.07N, \tag{11}$$

$$V_{cur,ACI} = \rho_v f'_{yv} \frac{A}{b} + \left(0.16\sqrt{f_c} + 17\rho_s \frac{V_{u1} A/b}{M_m}\right) A, \tag{12}$$

$$V_{cur,CSA} = \beta^* \sqrt{f_c} b d_v + \rho_v f'_{yv} d_v \cot\theta, \tag{13}$$

$$V_{gu} = \nu_g \rho_{sv} f_g b h_0, \tag{14}$$

$$V_{au} = \frac{0.58 f'_a t_w h_w}{\lambda - 0.2}. \tag{15}$$

4.3.2. Shear Strength Modes. Figure 8 shows the comparison of experimental and other methods from the ACI [24], the CSA [25], the GB (GB50010) [16], and proposed model. From Figure 8, the mean ratio and coefficient of variation are 1.43 and 0.24, 1.36 and 0.18, 1.13 and 0.16, and 1.07 and 0.13, respectively. The results indicate that the proposed model can predict the shear strength reasonably, and the code provisions are relatively conservative at the same time. The mean ratio of the GB50010 is about 1.0, which demonstrates that this code may tend to over-valuation of the shear strength. The predicted shear strength of the ACI318-08 and the CSA-04 is commonly conservative, because they neither consider the arch action nor base on the truss model and MCFT. As the shear span-depth ratio, λ, decreases, the conservative increases. The effect of arch action increases as the shear span-depth ratio, λ, decreases. It confirms that the proposed method is slightly conservative and safe.

5. Conclusions

Through the design and manufacture of four 1/2-scale SRC column models, the postearthquake damage, enveloped steel jacket-confined and destructive tests under lateral cyclic loading were carried out. The damage model, force-displacement relationship, deformation capacity, and shear strength are compared and discussed. Conclusions can be drawn after the tests and the predicted results comparison.

(1) Overall seismic behavior of strengthened columns was observed to be stronger compared with that of

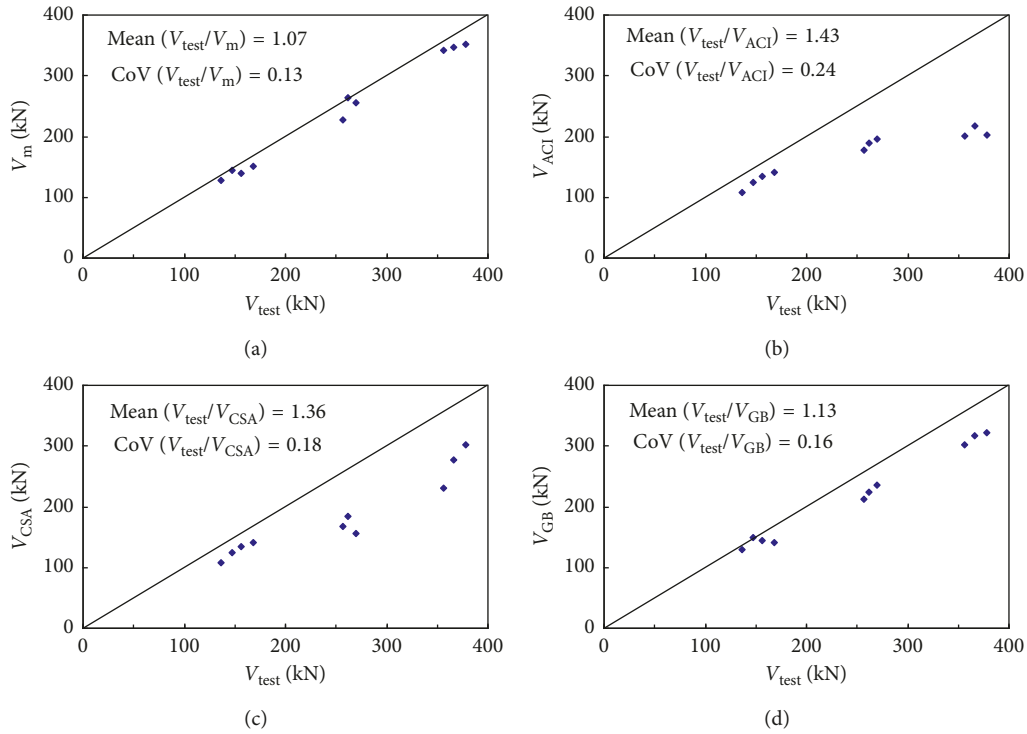

Figure 8: Comparison of experimental and other methods: (a) proposed model; (b) method in ACI318 (2008); (c) method in CSA (2004); (d) method in GB50010 (2010).

nonstrengthened column under the same conditions, displayed a relatively high ductility and energy dissipation capacity, and obtained higher shear capacity.

(2) Similar effect can be found between the enveloped steel jacket and the stirrups, which can effectively restrain the spalling of concrete cover at the bottom of the column and the increase of concrete cracks.

(3) Compared with the specimen SRC-0, the average of the ultimate load of the WSRC-0 increased by 23.0% and the average of the ultimate displacement increased by 23.7%; the average of the ultimate load of WSRC-1 increased by 12.9% and the average of the ultimate displacement increased by 12.4%; and the average of the ultimate load of WSRC-2 increased by 7.4% and the average of the ultimate displacement increased by 8.0%.

(4) The result of the prediction of shear strength is relatively conservative, because the arch action has been ignored by most code provisions. Thus, the condition of compatibility between seismic damage degree and enveloped steel jacket-confined needs to be considered.

Data Availability

The data used to support the findings of this study are available from the corresponding author upon request.

Conflicts of Interest

The authors declare no conflicts of interest.

Authors' Contributions

CW conceived and designed the experiments; SP performed the experiments and wrote the paper; and CX analyzed the data.

Acknowledgments

This research was funded by the National Natural Science Foundation of China (CN) (grant no. 51478048) and Natural Science Foundation of Hubei Province (Innovation Group) of China (CN) (grant no. 2015CFA029), and their support is gratefully acknowledged. Lastly, thanks to my girlfriend Fei Han's support and translation guidance.

References

[1] Z. Yang and C. X. Xu, "Research on compression behavior of square thin-walled CFST columns with steel-bar stiffeners," *Applied Sciences*, vol. 8, no. 9, pp. 1–11, 2018.

[2] C. X. Xu, B. Yang, B. Zhao, J. C. Zhang, and W. Peng, "Seismic performance of enveloped-steel-strengthened seismic-damaged CFST columns," *Journal of Guangxi University (Nat Soi Ed)*, vol. 40, no. 4, pp. 821–830, 2015, in Chinese.

[3] S. H. Park, D. J. Kim, G. S. Ryu, and K. T. Koh, "Tensile behavior of ultra high performance hybrid fiber reinforced

concrete," *Cement and Concrete Composites*, vol. 34, no. 2, pp. 172–184, 2012.

[4] C. Alessandri and J. Turrioni, "The church of the nativity in bethlehem: analysis of a local structural consolidation," *Cement and Concrete Composites*, vol. 34, no. 2, pp. 172–184, 2012.

[5] R. Jünemann, J. C. D. Llera, M. A. Hube, L. Cifuentes, and E. Kausel, "A statistical analysis of reinforced concrete wall buildings damaged during the 2010 Chile earthquake," *Engineering Structures*, vol. 82, pp. 168–185, 2018.

[6] K. Sadeghi and F. Nouban, "A highly accurate algorithm for nonlinear numerical simulation of RC columns under biaxial bending moment and axial loading applying rotary oblique fiber-element discretization," *International Journal of Civil Engineering*, vol. 16, no. 1, pp. 1–13, 2017.

[7] S. Karimiyan, A. S. Moghadam, A. Husseinzadeh Kashan, and M. Karimiyan, "Evaluation of collapse distribution in three-story RC moment-resisting asymmetric buildings due to earthquake loads," *International Journal of Civil Engineering*, vol. 15, no. 5, pp. 809–825, 2017.

[8] M. Remki, A. Kibboua, D. Benouar, and F. Kehila, "Seismic fragility evaluation of existing RC frame and URM buildings in Algeria," *International Journal of Civil Engineering*, vol. 16, no. 7, pp. 1–12, 2017.

[9] X. L. Chen, J. P. Fu, F. Xue, and X. F. Wang, "Comparative numerical research on the seismic behavior of RC frames using normal and high-strength reinforcement," *International Journal of Civil Engineering*, vol. 15, no. 4, pp. 531–547, 2017.

[10] C. X. Xu, L. Zeng, Q. Zhou, X. Tu, and T. Wu, "Cyclic performance of concrete-encased composite columns with T-shaped steel sections," *International Journal of Civil Engineering*, vol. 13, no. 4, pp. 456–467, 2015.

[11] M. E. Compagnoni and O. Curadelli, "Experimental and numerical study of the response of cylindrical steel tanks under seismic excitation," *International Journal of Civil Engineering*, vol. 16, no. 7, pp. 1–13, 2017.

[12] P. Nagaprasad, D. R. Sahoo, and D. C. Rai, "Seismic strengthening of RC columns using external steel cage," *Earthquake Engineering and Structural Dynamics*, vol. 38, no. 14, pp. 1563–1586, 2010.

[13] J. Garzón-Roca, J. Ruiz-Pinilla, J. M. Adam, and P. A. Calderón, "An experimental study on steel-caged RC columns subjected to axial force and bending moment," *Engineering Structures*, vol. 33, no. 2, pp. 580–590, 2011.

[14] C. D. Zhou, T. Tian, X. L. Lv, X. B. Bai, and H. Li, "Test study on seismic performance of pre-damaged RC cylinder piers strengthened with pre-stressed FRP belts," *Journal of the China Railway Society*, vol. 34, no. 10, pp. 103–114, 2012, in Chinese.

[15] L. Fang, B. Zhang, G.-F. Jin, K.-W. Li, and Z.-L. Wang, "Seismic behavior of concrete-encased steel cross-shaped columns," *Journal of Constructional Steel Research*, vol. 109, pp. 24–33, 2015.

[16] GB50010–2010, Code for design of concrete structures, 2015.

[17] JGJ 138–2001, Technical Specification for Steel Reinforced Concrete Composite Structures, 2001.

[18] C. X. Xu, S. Peng, J. Deng, and C. Wan, "Study on seismic behavior of encased steel jacket-strengthened earthquake-damaged composite steel-concrete columns," *Journal of Building Engineering*, vol. 17, pp. 154–166, 2018.

[19] R. M. Oinam and D. R. Sahoo, "Rehabilitation of damaged RC frames using combined metallic yielding passive devices," *Structures and Infrastructures Engineering*, vol. 13, no. 6, pp. 816–830, 2016.

[20] S. Peng, C. X. Xu, M. X. Lu, and J. M. Yang, "Experimental research and finite element analysis on seismic behavior of CFRP-strengthened seismic-damaged composite steel-concrete frame columns," *Engineering Structures*, vol. 155, pp. 50–60, 2018.

[21] L. Zhu, K. J. Elwood, and T. Haukaas, "Classification and seismic safety evaluation of existing reinforced concrete columns," *Journal of Structural Engineering*, vol. 133, no. 9, pp. 1316–1330, 2007.

[22] J. P. Wei and X. H. Zhang, "Analysis on the shear bearing capacity of solid-webbed steel reinforced concrete short column based on trussed arch model," *Progress of Steel Building Structure*, vol. 13, no. 4, pp. 52–56, 2011.

[23] Y. Y. Lu, L. Liu, H. Zhang, and H. J. Zhang, "Calculation method of sheer capacity of rc column combination strengthened with angle steel And CFRP," *Engineering Mechanics*, vol. 25, no. 5, pp. 157–162, 2008.

[24] ACI Committee 318, *Building Code Requirements for Structural Concrete and Commentary*, American Concrete Institute, Farmington Hills, MI, USA, 2008.

[25] CSA A. 23.3–04, Design of concrete structures, 2004.

[26] J. M. Yang, *Finite Element Analysis on Seismic Performance of Repaired and Strengthened Seismic-damaged Steel Reinforced Concrete Frame Columns*, Wuhan University of Science and Technology, Wuhan, China, 2017.

[27] L. P. Ye, S. H. Zhao, Q. W. Li, Q. R. Yue, and K. Zhang, "Calculation of shear strength of concrete column strengthened with carbon fiber reinforced plastic sheet," *J of Build Struct, ASCE*, vol. 21, no. 2, pp. 59–67, 2000.

[28] J. B. Manderh, M. J. Priestley, and R. Park, "Theoretical stress-strain model for confined concrete," *Journal of Structural Engineering*, vol. 114, no. 8, pp. 90–95, 1988.

[29] M. X. Lu, *Experimental Research on Seismic Behavior of CFRP-Strengthened Seismic-Damaged SRC Columns*, Yangtze University, Jingzhou, China, 2017.

[30] Y. F. Zhang, *Experimental Research on the Seismic Performance of Damaged Reinforced Concrete Columns Strengthened with Carbon Fiber Reinforced Plastics*, Mongolian University of Science and Technology, Ulan Bator, Mongolia, 2009.

[31] J. D. Liu, *Research on Modeling of Hysteretic Characteristics of RC Frames Damaged During Earthquake*, Chongqing University, Chongqing, China, 2015.

[32] Y. J. Park and H. S. Ang, "Mechanistic seismic damage model for reinforced concrete," *Journal of Structural Engineering*, vol. 111, no. 4, pp. 722–739, 1985.